Kendomycin Cytotoxicity against Bacterial, Fungal, and Mammalian Cells Is Due to Cation Chelation

Tranter, Dale

2020-04-24

Tranter , D , Filipuzzi , I , Lochmann , T , Knapp , B , Kellosalo , J , Estoppey , D , Pistorius , D , Meissner , A , Paavilainen , V O & Hoepfner , D 2020 , ' Kendomycin Cytotoxicity against Bacterial, Fungal, and Mammalian Cells Is Due to Cation Chelation ' , Journal of Natural Products , vol. 83 , no. 4 , pp. 965-971 . https://doi.org/10.1021/acs.jnatprod.9b00826

http://hdl.handle.net/10138/320332
https://doi.org/10.1021/acs.jnatprod.9b00826

JOURNAL OF NATURAL PRODUCTS

pubs.acs.org/jnp

Article

Kendomycin Cytotoxicity against Bacterial, Fungal, and Mammalian Cells Is Due to Cation Chelation

Dale Tranter,[§] Ireos Filipuzzi,[§] Thomas Lochmann, Britta Knapp, Juho Kellosalo, David Estoppey, Dominik Pistorius, Axel Meissner, Ville O. Paavilainen,* and Dominic Hoepfner*

Cite This: *J. Nat. Prod.* 2020, 83, 965−971

Read Online

ACCESS | Metrics & More | Article Recommendations | Supporting Information

ABSTRACT: Kendomycin is a small-molecule natural product that has gained significant attention due to reported cytotoxicity against pathogenic bacteria and fungi as well as a number of cancer cell lines. Despite significant biomedical interest and attempts to reveal its mechanism of action, the cellular target of kendomycin remains disputed. Herein it is shown that kendomycin induces cellular responses indicative of cation stress comparable to the effects of established iron chelators. Furthermore, addition of excess iron and copper attenuated kendomycin cytotoxicity in bacteria, yeast, and mammalian cells. Finally, NMR analysis demonstrated a direct interaction with cations, corroborating a close link between the observed kendomycin polypharmacology across different species and modulation of iron and/or copper levels.

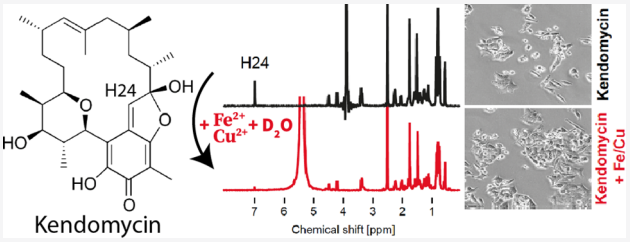

Natural products serve as privileged chemical probes for interrogating cellular biology, expanding the druggable genome, and eventually developing new therapeutics. The secondary metabolite kendomycin (Figure 1A) is a macrocyclic polyketide produced by several *Streptomyces* species. Since its discovery, a variety of cytotoxic activities, including killing of both Gram-negative and -positive bacteria,[1] pathogenic fungi,[2] and a number of human cancer cell lines,[2] were reported. This generated substantial interest in kendomycin, leading to the establishment of a total synthesis method[3] and identification and cloning of its corresponding polyketide synthase cluster.[4] Kendomycin was proposed to inhibit yeast and mammalian proteasomes,[5] but whereas a specific covalent interaction was reported, binding site mutations that abolished the interaction failed to alter kendomycin cytotoxicity.[5] Conservation of cytotoxic activity from bacteria to man may be indicative of either a highly conserved protein target or interference with common biomolecules such as nucleic acids, lipids, or ions. It was the aim of this study to identify the mechanism of action of kendomycin and thereby explain its pan-species activity.

RESULTS AND DISCUSSION

Kendomycin was previously characterized as a weak inhibitor of yeast and mammalian proteasomes.[5] To test whether proteasome inhibition plays a role in kendomycin cytotoxicity in human cells, a FACS-based proteasomal degradation assay was used that monitors cellular turnover of a destabilized UbG76V-GFP reporter as a measure of proteasome activity.[6] As expected, treating cells with the established proteasome inhibitor MG132 resulted in cellular accumulation of GFP. However, kendomycin failed to increase cellular GFP fluorescence even at acutely cytotoxic concentrations (Figures 1B and S1, Supporting Information), suggesting direct proteasome inhibition is not likely the primary mechanism of action of kendomycin.[2]

Kendomycin has been shown to affect the uptake of radiolabeled isoleucine in bacteria, indicative of protein synthesis inhibition.[7] To investigate the proposed kendomycin mechanism of action in mammalian cells, metabolic labeling of HCT116 cells with ^{35}S methionine/cysteine was used. As expected, treatment with an established ribosomal inhibitor cycloheximide abolished all protein synthesis, while the Sec61 translocation inhibitor apratoxin A[8] prevented biogenesis only of newly labeled secretory proteins. In contrast to cycloheximide or apratoxin A, kendomycin did not influence production of total or secretory proteins (Figure 1C). Therefore, inhibition of protein biogenesis is also not a likely primary mechanism by which kendomycin exerts its cytotoxic effect across a range of species.

Mutations at the target binding site of cytotoxic compounds can interfere with compound binding without affecting target functionality, and isolation and characterization of such resistance-conferring point mutations is the method of choice for identifying targets of cytotoxic compounds.[9−11] Given the broad cytotoxic range of kendomycin, both yeast and

Received: August 29, 2019
Published: March 17, 2020

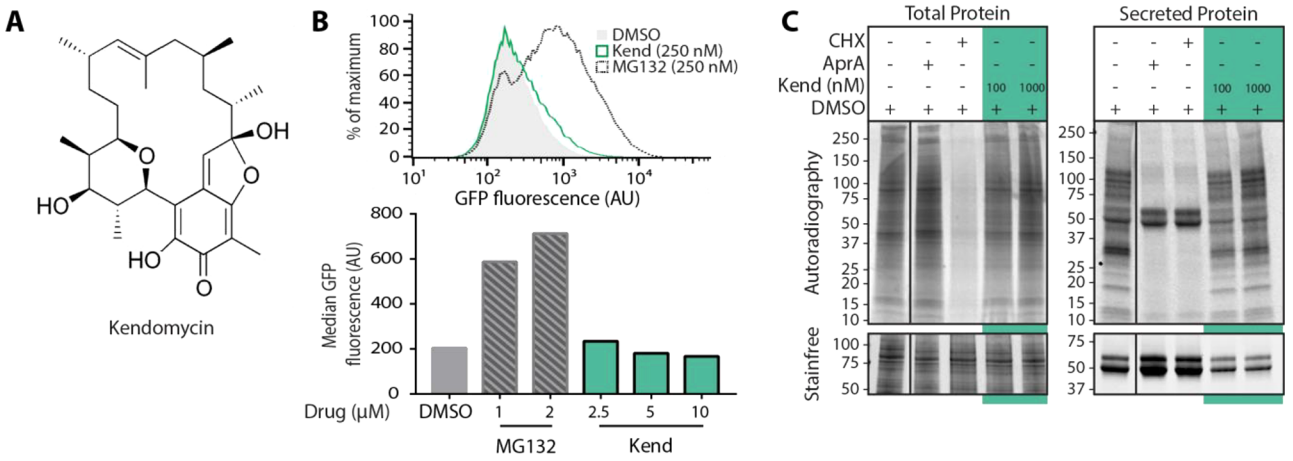

Figure 1. Kendomycin toxicity is not concurrent with proteostatic perturbations. (A) Structure of kendomycin. (B) Kendomycin treatment does not inhibit proteasome activity in mammalian cells. Fluorescence distribution of DMSO (gray infill), 250 nM MG132 (black), and 250 nM kendomycin (green) treated HEK293T cells expressing UbG76V-GFP proteosomal reporter and quantification from S1, Supporting Information. (C) HCT-116 cells grown in the presence of indicated concentrations of kendomycin, apratoxin A (inhibitor of the Sec61 protein translocon), or cycloheximide (protein synthesis inhibitor) and ^{35}S-labeled methionine/cysteine. Total protein shows cellular lysate; secreted protein shows the contents of the growth medium following TCA precipitation. As expected, cycloheximide inhibits protein biogenesis in both total and secreted fractions, while apratoxin A inhibits biogenesis of only secreted proteins. Kendomycin has no effect on biogenesis of either total or secreted fractions.

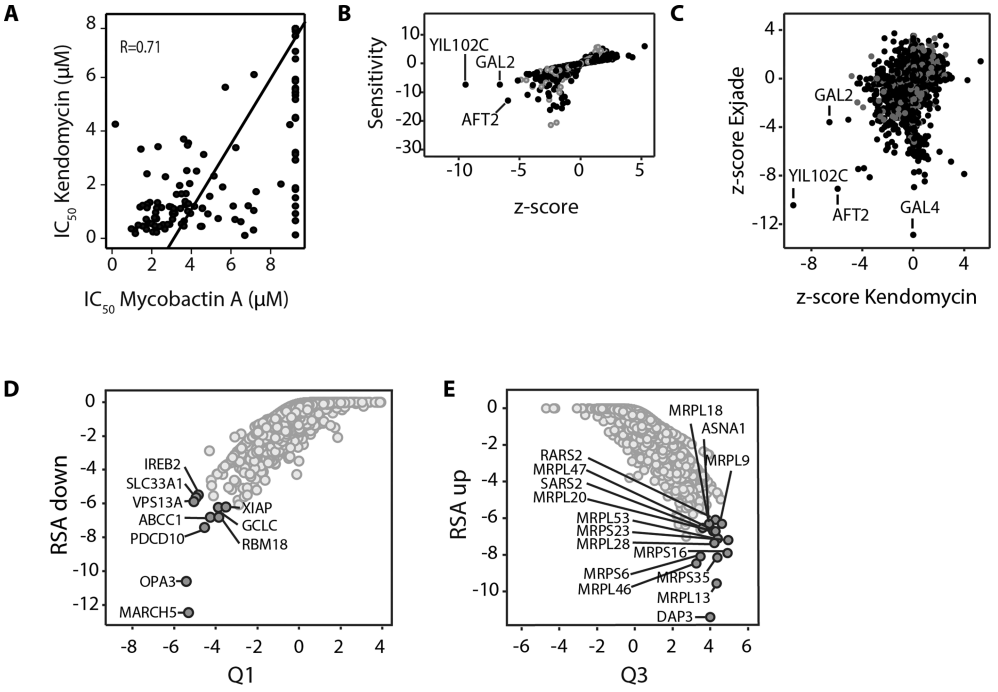

Figure 2. Chemogenomic profiling identifies a conserved link between iron dependence and kendomycin sensitivity. (A) The IC_{50} values of kendomycin are plotted against those of mycobactin A, resulting in a Pearson correlation coefficient (R) of 0.71, suggesting that kendomycin might utilize a similar mechanism of action to the bacterial siderophore. (B) HIP profile of kendomycin tested in two independent biological replicates at 16.5 μM. Sensitivity of the heterozygous deletion strains is plotted against statistical significance (z-score) as previously described.[1] Black dots represent nonessential and gray squares essential genes of the *S. cerevisiae* genome. Alignment of the z-scores of kendomycin and the clinical cation chelator exjade reveals a conserved set of hypersensitive hits, shown in (C), providing further evidence that kendomycin shares a similar mechanism of action with cation chelators in general. The relative gene-level depletion (D) and the enrichment (E) scores from an inhibitor-sensitized CRISPR screen of kendomycin at 400 nM in HCT116 cells are shown. The RSA p-value, a gene-level measure for conserved depletion (RSA down) or enrichment (RSA up) of its respective guides, is plotted against Q, a gene-level effect size corresponding to the RSA p-value for depletion (Q1) or enrichment (Q3). The most significant hits reveal an abundance of iron interactive processes.

mammalian cells were randomly mutagenized by ethyl methanesulfonate and screened for permissive kendomycin-resistant mutants. In total, 48 *Saccharomyces cerevisiae* colonies were isolated, grown to saturation in the absence of drug, and then replated on agar supplemented with kendomycin. However, no resistance was observed to persist in any clones using this approach, indicating that initial resistance was obtained through adaptation rather than mutation. Analo-

https://dx.doi.org/10.1021/acs.jnatprod.9b00826
J. Nat. Prod. 2020, 83, 965−971

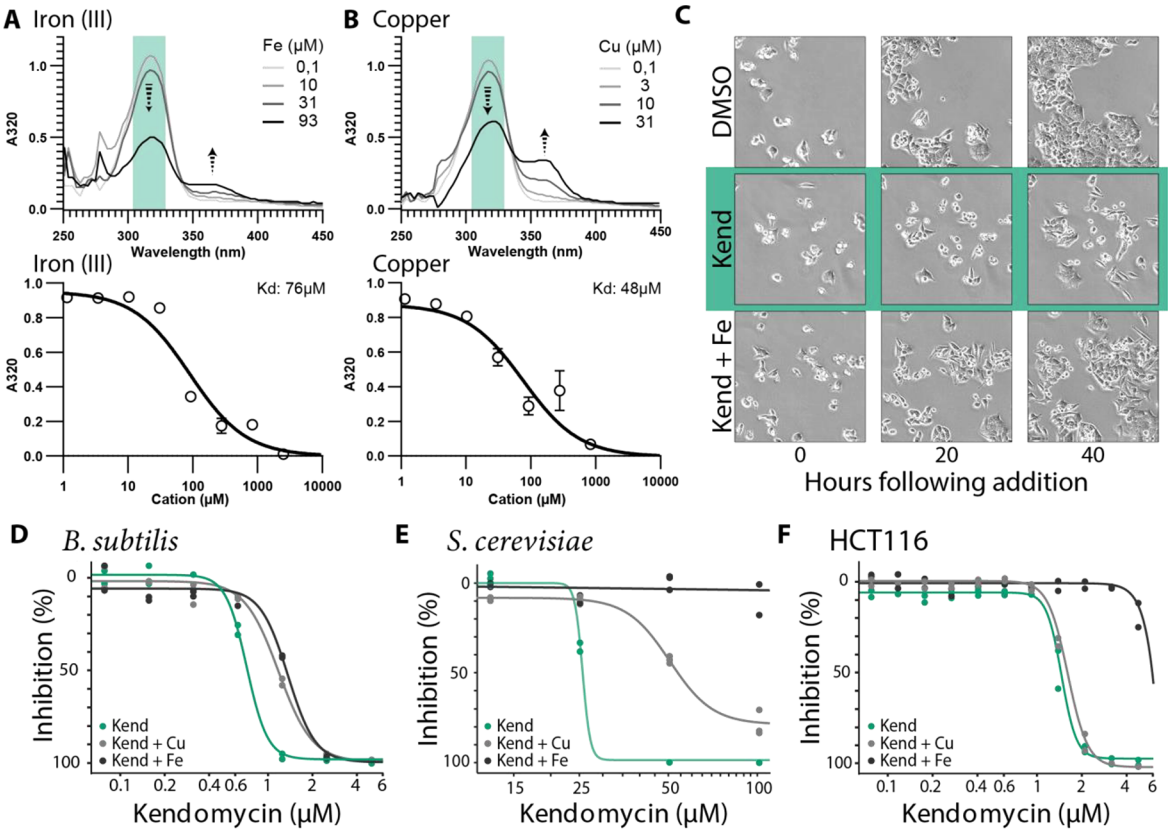

Figure 3. Exogenous cations ameliorate kendomycin cytotoxicity across species. Spectra of 250 μM kendomycin with increasing concentrations of iron (A) or copper (B). A_{320} were measured in quadruplicate, and average values used to estimate a binding curve for each (A and B, bottom), from which K_{app} was determined. (C) Kinetics of kendomycin toxicity and rescue by supplementation with 0.5 mM $FeCl_2$ in HCT116 cells. Cell proliferation in the presence of kendomycin is halted at 10 h, while Fe(II) supplementation allows continued proliferation. Dose−response curves of kendomycin were performed in the presence and absence of (D) 0.25 mM $FeCl_2$ and 0.25 mM $CuCl_2$ against *B. subtilis*, (E) 1 mM $FeCl_2$ and 0.25 mM $CuCl_2$ against *S. cerevisiae* on solid medium, and (F) 0.5 mM $FeCl_2$ and 0.5 mM $CuCl_2$ against HCT116 cells in duplicate, and inhibition curves were fitted by regression. Shift in the dose−response curves indicates that cation supplementation ameliorates kendomycin toxicity under these conditions.

gously, 18 resistant clonal HCT116 cell lines were identified that were subjected to whole-genome sequencing. The resulting SNP data identified many mutations, but none of these were enriched at particular genes or cellular pathways (Table S1, Supporting Information). Together, these results are in accordance with an earlier global proteomic response study,[2] which identified numerous kendomycin-modulated proteins spreading throughout multiple diverse biological processes, but lacking an obvious functional connection. Together, these results suggest that the target of kendomycin may not be a valid target of mutagenesis.

To identify the mechanism of action of kendomycin by an alternative unbiased approach, it was assayed against the Cancer Cell Line Encyclopedia, a collection of 512 human cancer cell lines (broadinstitute.org/ccle) with established sensitivities to a host of drug-like small molecules.[12] When querying the distribution of antiproliferative IC_{50} values against the tested compounds, the closest correlation with kendomycin (R = 0.71) was observed with the iron-chelating siderophore mycobactin A12 (Figure 2A), despite a lack of structural similarity between the two compounds. This prompted the hypothesis that kendomycin may exert its cytotoxic effect by cation modulation. Thus, it was attempted to assess kendomycin impact on yeast cells in an unbiased, genome-wide manner by chemogenomic haploinsufficiency profiling (HIP), a gene dosage-dependent method that assesses the effect of compounds against *S. cerevisiae* targets and pathways[13] and can also reveal compound mechanisms not directly targeting a protein.[14,15] Consistent with the hypothesis that kendomycin might act through a nonprotein target, the HIP profile of kendomycin did not reveal strongly affected heterozygous deletion strains (Figure 2B). The most pronounced effect was observed in a heterozygous deletion of *AFT2*, an iron-regulated transcriptional activator that activates genes involved in iron homeostasis.[16] Weaker, but still statistically significant hits included a heterozygous deletion of an uncharacterized ORF *YIL102C*, reported to be sensitive to Al(III),[17] and the galactose permease *GAL2*. When correlating this profile to our database of >3000 HIP profiles, an overlap of hits with the clinical cation chelator Exjade was apparent (Figure 2C), providing further experimental support for cation modulation by kendomycin.

A similar chemogenomic profiling experiment was performed in human cells using CRISPR/Cas9-mediated gene attenuation, as previously published.[18] The obtained sequencing data were plotted to identify genes for which the modulation can confer hypersensitivity (Figure 2D) or hyper-resistance (Figure 2E). Genes that conferred hypersensitivity against kendomycin were the mitochondrial E3 ubiquitin ligase MARCH5, involved in stress-induced apoptosis,[19] and the mitochondrial membrane protein OPA3, reported to exert cell-protective functions.[20] Weaker, but

https://dx.doi.org/10.1021/acs.jnatprod.9b00826
J. Nat. Prod. 2020, 83, 965−971

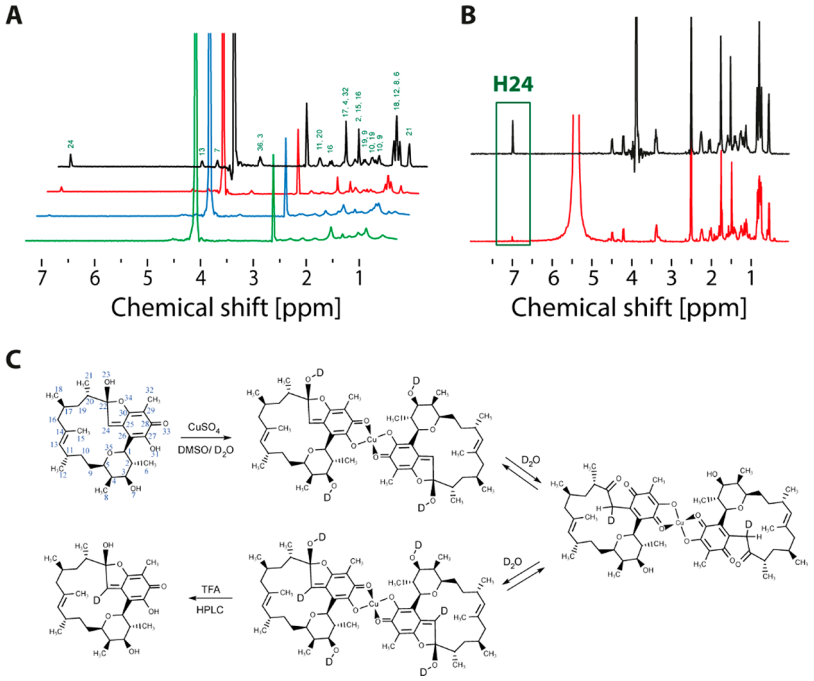

Figure 4. Kendomycin cation binding. (A) ^{1}H NMR spectra of 4 mM kendomycin with increasing concentrations of $CuSO_4$: 0 (black), 0.33 (red), 0.66 (blue), and 1 equivalent (green). See Figure S3 in the Supporting Information for complete chemical shift assignments. (B) ^{1}H NMR spectra of kendomycin (black) and of kendomycin treated with 1 equivalent of aqueous $CuSO_4$ and quenched after 1 day with TFA (red) prior to analysis. Protected peak is indicative of the copper interaction site. (C) Proposed kendomycin Cu(II) complex and potential mechanism for H/D exchange (axial water not shown for better representation).

statistically significant hits included the iron responsive element binding protein 2, IREB2, the ABC transporter ABCC1, which transports dinitrosyl-dithiol-iron complexes,[21] GCLC, the rate-limiting enzyme of glutathione synthesis essential for iron−sulfur cluster formation,[22] and XIAP, the iron- and copper-dependent X-linked inhibitor of apoptosis.[23,24] Most of the mammalian hypersensitive hits were directly linked to iron metabolism or were closely connected to iron-dependent processes. The hits conferring hyper-resistance exclusively comprised genes directly linked to mitochondrial protein synthesis such as subunits of the mito-ribosome and different tRNA synthetases. Mitochondria, the major consumers of cellular iron, are dispensable in the high-glucose medium routinely used in mammalian tissue culture, reducing cellular iron demand.[20] This may explain the frequency of iron metabolism-regulating genes in the resistance profile. Taken together, the data obtained from yeast and mammalian cells support interference of kendomycin with iron-dependent processes.

Next, it was desired to test whether addition of exogenous iron or other cations could modulate kendomycin activity. Mixing kendomycin with iron or copper in a test tube resulted in a concentration-dependent color change suggestive of a direct interaction (Figure S2, Supporting Information). Importantly, no color change was observed with other cations, including calcium, cobalt, magnesium, or manganese, indicative of highly selective cation chelation. To quantitatively determine relative affinities for kendomycin toward different physiologically relevant cations, an absorbance-based assay was used. The characteristic A_{320} nm absorbance peak of kendomycin was effectively quenched by addition of selected cations Fe(II), Fe(III), or Cu(II) (Figure 3A and B, Figure S2, Supporting Information). Conversely, addition of Ca^{2+} or Mg^{2+} did not cause any detectable changes in the UV spectra, suggesting a lack of interaction with these cations (Figure S2, Supporting Information). Modeling the concentration-dependent quenching allowed determination of kendomycin affinities toward different cations. Based on this analysis, the apparent kendomycin affinities were K_{app} 19 μM (Fe(II)), 48 μM (Cu(II)), and 76 μM (Fe(III)), with no observed binding for calcium or magnesium. Further, supplementing cultures of *B. subtilis* (Figure 3D), *S. cerevisiae* (Figure 3E), or human HCT116 colon carcinoma cells (Figures 3C and F) with iron partially alleviated cytotoxicity in all three species, consistent with the essential role of iron for viability of all forms of life.[25] In contrast, copper rescued kendomycin cytotoxicity only in bacteria and yeast under these conditions, possibly reflecting the mechanisms that these species use to tightly regulate free copper and mitigate its antimicrobial effect.[26]

Having established a plausible link between cation availability and kendomycin cytotoxicity, it was sought to demonstrate direct cation binding. To test this, the complete chemical shift assignment of kendomycin using 1D and 2D NMR approaches was determined (Figure S3, Supporting Information) followed by measurements in the presence of different cations. Addition of iron(II) or copper(II) resulted in a dose-dependent shift and broadening of the NMR signals (Cu(II) Figure 4A; Fe(II) Figure S4, Supporting Information) and a decreased overall intensity of kendomycin signals. Based on the magnitude of the paramagnetic effect of the metal ions, we were able to derive a rough epitope mapping[27] indicating the 2,5-dihydroxy-7-methyl-1-benzofuran-6(2*H*)-one moiety as the metal ion binding site (Figure 4C). In order to prove the presence of a coordination complex and to rule out redox-based mechanisms, the kendomycin−copper complex was quenched with TFA, reverting the ^{1}H NMR spectrum to one

https://dx.doi.org/10.1021/acs.jnatprod.9b00826
J. Nat. Prod. 2020, 83, 965−971

identical to the parent compound with only H-24 missing (Figure 4B).

LC-MS experiments of the TFA-quenched complex indicated that the lack of this signal can be attributed to H/D exchange (Figure S4, Supporting Information). Using time-dependent quenching experiments, we could show that the H/D exchange occurs with an approximate rate constant of $k \approx 0.06\ h^{-1}$ (Figure S5, Supporting Information). Since no H/D exchange was observed in the absence of copper or iron ions, it was postulated that the underlying mechanism is linked to the metal binding mode in the complex. Assuming a geometry similar to other hydroxyquinone copper(II) complexes,[28] a 2:1 stoichiometry with a bidentate kendomycin ligand can be proposed. This binding mode could explain the observed H/D exchange via an opening of the hemiketal in equilibrium (Figure 4C). Other molecular mechanisms such as proton-coupled electron transfer for the quinone ligand might be included but were not resolved with the experimental setup used in this study.

In summary, genome-wide and focused data sets generated in yeast and mammalian cells, as well as molecular data, all indicate that the reported activities of kendomycin are attained by sequestration of iron and copper. Since iron is vital for all phyla, this also explains the pan-species activity of kendomycin. Oxidative stress and cation imbalance are linked to many diseases, and chelating natural products such as curcumin and gossypol[29−31] or salinomycin,[32] which sequesters lysosomal iron, have accepted clinical benefits. This report thus provides a direction for further, focused investigations of clinical applications of kendomycin.

EXPERIMENTAL SECTION

General Experimental Procedures. Kendomycin was isolated from an unclassified Actinomycetes strain grown in a submerged culture. A crude extract was generated by extraction of the culture broth with ethyl acetate, and kendomycin was purified by subsequent normal-phase and reversed-phase chromatographic separations. The final purity was assessed by HPLC coupled to UV−vis, MS, and charged aerosol detectors and found to be at least 97%.

Effects of the Proteasome Inhibitor MG132 and Kendomycin on Cellular Turnover of a Destabilized Ub^{G76V}-GFP Reporter. K562 cells bearing the lentivirally integrated ubiquitin fusion degradation reporter Ub^{G76V}-GFP[6] controlled by an inducible TRE2 promoter were induced 16 h prior to addition of compounds by adding doxycycline to a final concentration of 1 μg/mL. Induced cells were treated with the indicated compounds or carrier for 4 h, then analyzed by flow-cytometry on a BD LSRFortessa instrument (BD Biosciences).

Metabolic Labeling. HCT116 cells were seeded onto six-well plates (0.5×10^6 cells/well) and then incubated at 37 °C at 5% CO_2 for 24 h. Cells were washed twice, and 1 mL of compound diluted in DMEM lacking methionine and cysteine was added to each well. The plate was then incubated at 37 °C for 30 min prior to addition of 100 μCi ^{35}S-labeled methionine/cysteine (Expre^{35}s^{35}s protein labeling mix). Plates were incubated for a further 90 min; then medium was collected and cells were harvested by scraping after four washes in ice-cold PBS. Total protein was acquired by RIPA extraction from the cell pellet, and secreted proteins were acquired by TCA precipitation of the medium. Gel-exposed storage phosphor screens were scanned on a Typhoon 9400 variable-mode imager.

EMS Mutagenesis. Strain BY4743Δ8, derived from BY4741 but deleted for eight genes involved in drug resistance (efflux pumps: *SNQ2*, *PDR5*, *YOR1*; transcription factors: *PDR1*, *PDR2*, *PDR3*, *YAP1*, *YRM1*), was incubated in 2.5% ethyl methanesulfonate until only 50% of the cells formed colonies. A total of 2×10^7 mutagenized cells were plated on two 14 cm dishes containing growth inhibitory concentrations of kendomycin. After 4 days, resistant colonies could be isolated and were restreaked onto selective plates. Detailed experimental procedures were followed as described.[33]

Chemogenetic Screening. HCT116 cells were grown in McCoy's 5A medium supplemented with 10% fetal bovine serum (FBS). EMS-mutagenized and untreated cells were seeded in 10 cm dishes at a density of 0.5×10^6 cells/dish. Then, 24 h after plating the medium was removed and replaced with media containing a range of concentrations of the compound. Selection was maintained for 14 days by replacement of medium and compound every 48−72 h. Colonies were isolated from selection plates at an uppermost selection concentration of 2 μM kendomycin. Resistance of isolated cell lines to a panel of cytotoxic compounds compared to the parental pool of HCT116 cells and cell lines showing generalized increase in resistance were discarded. In total 18 cell lines showing mild resistance to kendomycin were obtained, eight of which were derived from cells that were treated with EMS 24 h prior to initiation of selection as described.[34] Confirmed cell lines were then subjected to whole-genome sequencing.

Chemogenomic Profiling. Yeast haploinsufficiency profiling,[14] measuring individual kendomycin hypersensitivity of a genome-wide collection of heterozygous deletion strains relative to the isogenic wild-type; CRISPR profiling, measuring hypersensitivity of HCT116 mammalian cells transduced with a genome-wide sgRNA library resulting in editing of all annotated protein-coding genes;[18] and CCLE profiling,[10] measuring IC_{50} curves of cytotoxic compounds against the Cancer Cell Line Encyclopedia, were performed as described.

Bacterial Growth Inhibition. Mid logarithmic *B. subtilis* cultures in LB medium samples were back-diluted to low optical density, and 125 μL of cultures was dispensed with an electronic multichannel pipet into a 96-well plate. Then, 5 μL from an 8-point kendomycin serial dilution series was added to the wells of six columns to allow for data sets in duplicates. Two columns were supplemented with freshly prepared 0.25 mM $FeCl_2$ or 0.25 mM $CuCl_2$, respectively. Plates were incubated at 37 °C with 1000 rpm orbital shaking, and cell densities determined by A_{600}.

Yeast Growth Inhibition. Single-colony inhibition was performed as described.[33] Colonies were then washed off the plates with 1 mL of PBS, and cell densities determined by A_{600} measurement.

Mammalian Growth Inhibition. HCT-116 cells were maintained at 37 °C, 5% CO_2 in McCoy's 5A medium supplemented with 10% FBS. For cell proliferation assays, cells were seeded in 96-well viewplates (PerkinElmer, cat. no. 6005182) at a density of 2500 cells/well. Then, 16 h after plating the cells were treated with the indicated compounds or carrier. Next, 72 h after compound dosing the medium was supplemented with 10% Alamar Blue (resazurin) and the cells were returned to the incubator for a further 4 h. Fluorescence intensity (excitation 580 nm, emission 620 nm) was measured using a microplate reader (PerkinElmer EnSpire). Viability was calculated as a percentage of maximal growth under carrier, and dose−response curves were calculated using GraphPad Prism 7. Dose−response curves were calculated from quadruplicate technical replicates.

For cell imaging time courses, cells were seeded in 24-well imaging plates (Nunc Nunclon-treated multiwell dishes) at a density of 25 000 cells/well. Then, 16 h after plating, the cells were treated with indicated compounds or carrier. Immediately following dosing, plates were loaded into a precalibrated CellIQ continuous cell culturing platform. Cultures were imaged at 3 points per condition every 10 min for 48 h.

NMR Analysis. Standard 1D and 2D NMR methodology was applied for structure elucidation and titration experiments. For NMR spectral assignment, 0.4 mg of kendomycin was dissolved in 500 μL of DMSO-d_6/D_2O (80%:20% v/v). The obtained clear solution was transferred into a 5.0 mm NMR sample tube for measurement. ^{1}H and ^{13}C detected 1D and 2D NMR spectra of the sample were recorded at 300 K using a Bruker 600 MHz AVANCE III HD spectrometer equipped with a 5.0 mm ^{13}C{^{1}H} CryoProbe with a *z*-gradient system. For titration experiments 1.0 mg of kendomycin was dissolved in 600 μL of DMSO-d_6/D_2O (85%:15% v/v) in the

https://dx.doi.org/10.1021/acs.jnatprod.9b00826
J. Nat. Prod. 2020, 83, 965−971

presence of 0.33, 0.66, and 1.0 equiv of either $CuSO_4$ or $FeSO_4$. The obtained orange to dark red solutions were transferred into 5.0 mm NMR sample tubes prior to acquisition. ^1H NMR data were recorded at 300 K using a Bruker 500 MHz AVANCE III spectrometer equipped with a 5 mm BBO probe with a *z*-gradient system. All spectra were referenced according to the internal solvent signal (^1H: DMSO = 2.50 ppm and ^{13}C: DMSO = 39.5 ppm).

■ ASSOCIATED CONTENT

Supporting Information

The Supporting Information is available free of charge at https://pubs.acs.org/doi/10.1021/acs.jnatprod.9b00826.

Additional information (PDF)

■ AUTHOR INFORMATION

Corresponding Authors

Ville O. Paavilainen − *Institute of Biotechnology, University of Helsinki, Helsinki 00014, Finland;* orcid.org/0000-0002-3160-7767; Phone: +358-50-448 4600; Email: ville.paavilainen@helsinki.fi

Dominic Hoepfner − *Novartis Institutes for BioMedical Research, 4056 Basel, Switzerland;* orcid.org/0000-0001-8450-7543; Phone: +41 79 863 45 24; Email: dominic.hoepfner@novartis.com

Authors

Dale Tranter − *Institute of Biotechnology, University of Helsinki, Helsinki 00014, Finland;* orcid.org/0000-0001-7757-5484

Ireos Filipuzzi − *Novartis Institutes for BioMedical Research, 4056 Basel, Switzerland;* orcid.org/0000-0002-2493-6183

Thomas Lochmann − *Novartis Institutes for BioMedical Research, 4056 Basel, Switzerland*

Britta Knapp − *Novartis Institutes for BioMedical Research, 4056 Basel, Switzerland*

Juho Kellosalo − *Institute of Biotechnology, University of Helsinki, Helsinki 00014, Finland*

David Estoppey − *Novartis Institutes for BioMedical Research, 4056 Basel, Switzerland*

Dominik Pistorius − *Novartis Institutes for BioMedical Research, 4056 Basel, Switzerland*

Axel Meissner − *Novartis Institutes for BioMedical Research, 4056 Basel, Switzerland*

Complete contact information is available at: https://pubs.acs.org/10.1021/acs.jnatprod.9b00826

Author Contributions

[§]I. Filipuzzi and D. Tranter contributed equally to this work.

Notes

The authors declare the following competing financial interest(s): The authors declare that they have no conflicts of interest with the contents of this article. Authors with the affiliation Novartis Institutes for BioMedical Research are employees of Novartis and may have stock in the company.

■ ACKNOWLEDGMENTS

This work was supported by the Academy of Finland (grants 289737 and 314672), U.S. National Institutes of Health (Project 1R01GM132649-01), and the Sigrid Juselius Foundation. The content is solely the responsibility of the authors and does not necessarily represent the official views of the National Institutes of Health. The authors are grateful to Ralph Riedl and Thomas Aust for operating the HIP HOP platform, Sven Schuierer for support in yeast data, Florian Nigsch for mammalian data processing, Alicia Lindemann and Carsten Russ for sequencing support, John Reece-Hoyes for providing the lentiviral sgRNA library, and N. Ross for CLiP profiling. We acknowledge the use of the University of Helsinki HiLife Flow Cytometry Unit at the Faculty of Biological and Environmental Sciences.

■ REFERENCES

(1) Enkh-Amgalan, J.; Komaki, H.; Daram, D.; Ando, K.; Tsetseg, B. *J. Antibiot.* **2012**, *65*, 103−108.

(2) Elnakady, Y. A.; Rohde, M.; Sasse, F.; Backes, C.; Keller, A.; Lenhof, H.-P.; Weissman, K. J.; Müller, R. *ChemBioChem* **2007**, *8*, 1261−1272.

(3) Yuan, Y.; Men, H.; Lee, C. *J. Am. Chem. Soc.* **2004**, *126*, 14720−14721.

(4) Wenzel, S. C.; Bode, H. B.; Kochems, I.; Müller, R. *ChemBioChem* **2008**, *9*, 2711−2721.

(5) Beck, P.; Heinemeyer, W.; Späth, A.-L.; Elnakady, Y.; Müller, R.; Groll, M. *J. Mol. Biol.* **2014**, *426*, 3108−3117.

(6) Johnson, E. S.; Ma, P. C.; Ota, I. M.; Varshavsky, A. *J. Biol. Chem.* **1995**, *270*, 17442−17456.

(7) Elnakady, Y. A.; Chatterjee, I.; Bischoff, M.; Rohde, M.; Josten, M.; Sahl, H.-G.; Herrmann, M.; Müller, R. *PLoS One* **2016**, *11*, e0146165.

(8) Paatero, A. O.; Kellosalo, J.; Dunyak, B. M.; Almaliti, J.; Gestwicki, J. E.; Gerwick, W. H.; Taunton, J.; Paavilainen, V. O. *Cell Chem. Biol.* **2016**, *23*, 561−566.

(9) Filipuzzi, I.; Cotesta, S.; Perruccio, F.; Knapp, B.; Fu, Y.; Studer, C.; Pries, V.; Riedl, R.; Helliwell, S. B.; Petrovic, K. T.; Movva, N. R.; Sanglard, D.; Tao, J.; Hoepfner, D. *PLoS Genet.* **2016**, *12*, e1006374.

(10) Krastel, P.; Roggo, S.; Schirle, M.; Ross, N. T.; Perruccio, F.; Aspesi, P.; Aust, T.; Buntin, K.; Estoppey, D.; Liechty, B.; Mapa, F.; Memmert, K.; Miller, H.; Pan, X.; Riedl, R.; Thibaut, C.; Thomas, J.; Wagner, T.; Weber, E.; Xie, X.; Schmitt, E. K.; Hoepfner, D. *Angew. Chem., Int. Ed.* **2015**, *54*, 10149−54.

(11) Zuryn, S.; Jarriault, S. *Worm* **2013**, *2*, e25081.

(12) Barretina, J.; Caponigro, G.; Stransky, N.; Venkatesan, K.; Margolin, A. A.; Kim, S.; Wilson, C. J.; Lehár, J.; Kryukov, G. V.; Sonkin, D.; Reddy, A.; Liu, M.; Murray, L.; Berger, M. F.; Monahan, J. E.; Morais, P.; Meltzer, J.; Korejwa, A.; Jané-Valbuena, J.; Mapa, F. A.; Thibault, J.; Bric-Furlong, E.; Raman, P.; Shipway, A.; Engels, I. H.; Cheng, J.; Yu, G. K.; Yu, J.; Aspesi, P.; de Silva, M.; Jagtap, K.; Jones, M. D.; Wang, L.; Hatton, C.; Palescandolo, E.; Gupta, S.; Mahan, S.; Sougnez, C.; Onofrio, R. C.; Liefeld, T.; MacConaill, L.; Winckler, W.; Reich, M.; Li, N.; Mesirov, J. P.; Gabriel, S. B.; Getz, G.; Ardlie, K.; Chan, V.; Myer, V. E.; Weber, B. L.; Porter, J.; Warmuth, M.; Finan, P.; Harris, J. L.; Meyerson, M.; Golub, T. R.; Morrissey, M. P.; Sellers, W. R.; Schlegel, R.; Garraway, L. A. *Nature* **2012**, *483*, 603−607.

(13) Giaever, G.; Flaherty, P.; Kumm, J.; Proctor, M.; Nislow, C.; Jaramillo, D. F.; Chu, A. M.; Jordan, M. I.; Arkin, A. P.; Davis, R. W. *Proc. Natl. Acad. Sci. U. S. A.* **2004**, *101*, 793−798.

(14) Hoepfner, D.; Helliwell, S. B.; Sadlish, H.; Schuierer, S.; Filipuzzi, I.; Brachat, S.; Bhullar, B.; Plikat, U.; Abraham, Y.; Altorfer, M.; Aust, T.; Baeriswyl, L.; Cerino, R.; Chang, L.; Estoppey, D.; Eichenberger, J.; Frederiksen, M.; Hartmann, N.; Hohendahl, A.; Knapp, B.; Krastel, P.; Melin, N.; Nigsch, F.; Oakeley, E. J.; Petitjean, V.; Petersen, F.; Riedl, R.; Schmitt, E. K.; Staedtler, F.; Studer, C.; Tallarico, J. A.; Wetzel, S.; Fishman, M. C.; Porter, J. A.; Movva, N. R. *Microbiol. Res.* **2014**, *169*, 107−120.

(15) Lee, A. Y.; St Onge, R. P.; Proctor, M. J.; Wallace, I. M.; Nile, A. H.; Spagnuolo, P. A.; Jitkova, Y.; Gronda, M.; Wu, Y.; Kim, M. K.; Cheung-Ong, K.; Torres, N. P.; Spear, E. D.; Han, M. K. L.; Schlecht, U.; Suresh, S.; Duby, G.; Heisler, L. E.; Surendra, A.; Fung, E.; Urbanus, M. L.; Gebbia, M.; Lissina, E.; Miranda, M.; Chiang, J. H.; Aparicio, A. M.; Zeghouf, M.; Davis, R. W.; Cherfils, J.; Boutry, M.; Kaiser, C. A.; Cummins, C. L.; Trimble, W. S.; Brown, G. W.;

Schimmer, A. D.; Bankaitis, V. A.; Nislow, C.; Bader, G. D.; Giaever, G. *Science* **2014**, *344*, 208−211.
(16) Courel, M.; Lallet, S.; Camadro, J.-M.; Blaiseau, P.-L. *Mol. Cell. Biol.* **2005**, *25*, 6760−6771.
(17) Tun, N. M.; O'Doherty, P. J.; Perrone, G. G.; Bailey, T. D.; Kersaitis, C.; Wu, M. J. *Metallomics* **2013**, *5*, 1068−1075.
(18) Estoppey, D.; Hewett, J. W.; Guy, C. T.; Harrington, E.; Thomas, J. R.; Schirle, M.; Cuttat, R.; Waldt, A.; Gerrits, B.; Yang, Z.; Schuierer, S.; Pan, X.; Xie, K.; Carbone, W.; Knehr, J.; Lindeman, A.; Russ, C.; Frias, E.; Hoffman, G. R.; Varadarajan, M.; Ramadan, N.; Reece-Hoyes, J. S.; Wang, Q.; Chen, X.; McAllister, G.; Roma, G.; Bouwmeester, T.; Hoepfner, D. *Sci. Rep.* **2017**, *7*, 42728.
(19) Xu, S.; Cherok, E.; Das, S.; Li, S.; Roelofs, B. A.; Ge, S. X.; Polster, B. M.; Boyman, L.; Lederer, W. J.; Wang, C.; Karbowski, M. *Mol. Biol. Cell* **2016**, *27*, 349−359.
(20) Pei, W.; Kratz, L. E.; Bernardini, I.; Sood, R.; Yokogawa, T.; Dorward, H.; Ciccone, C.; Kelley, R. I.; Anikster, Y.; Burgess, H. A.; Huizing, M.; Feldman, B. *Development* **2010**, *137*, 2587−2596.
(21) Kovacevic, Z.; Sahni, S.; Lok, H.; Davies, M. J.; Wink, D. A.; Richardson, D. R. *Biochim. Biophys. Acta, Gen. Subj.* **2017**, *1861*, 995−999.
(22) Sen, S.; Cowan, J. A. *JBIC, J. Biol. Inorg. Chem.* **2017**, *22*, 1075−1087.
(23) Zuo, J.; Schmitt, S. M.; Zhang, Z.; Prakash, J.; Fan, Y.; Bi, C.; Kodanko, J. J.; Dou, Q. P. *J. Cell. Biochem.* **2012**, *113*, 2567−2575.
(24) Liang, Y.; Ewing, P. M.; Laursen, W. J.; Tripp, V. T.; Singh, S.; Splan, K. E. *J. Inorg. Biochem.* **2014**, *140*, 104−110.
(25) Andreini, C.; Bertini, I.; Cavallaro, G.; Holliday, G. L.; Thornton, J. M. *JBIC, J. Biol. Inorg. Chem.* **2008**, *13*, 1205−1218.
(26) Vincent, M.; Duval, R. E.; Hartemann, P.; Engels-Deutsch, M. *J. Appl. Microbiol.* **2018**, *124*, 1032−1046.
(27) Espersen, W. G.; Martin, R. B. *J. Am. Chem. Soc.* **1976**, *98*, 40−44.
(28) Salunke-Gawali, S.; Rane, S. Y.; Puranik, V. G.; Guyard-Duhayon, C.; Varret, F. *Polyhedron* **2004**, *23*, 2541−2547.
(29) Wang, X.-S.; Zhang, Z.-R.; Zhang, M.-M.; Sun, M.-X.; Wang, W.-W.; Xie, C.-L. *BMC Complementary Altern. Med.* **2017**, *17*, 412.
(30) Griffiths, K.; Aggarwal, B. B.; Singh, R. B.; Buttar, H. S.; Wilson, D.; De Meester, F. *Diseases* **2016**, *4*, 28.
(31) Dodou, K.; Anderson, R. J.; Small, D. A. P.; Groundwater, P. W. *Expert Opin. Invest. Drugs* **2005**, *14*, 1419−1434.
(32) Hamai, A.; Cañeque, T.; Müller, S.; Mai, T. T.; Hienzsch, A.; Ginestier, C.; Charafe-Jauffret, E.; Codogno, P.; Mehrpour, M.; Rodriguez, R. *Autophagy* **2017**, *13*, 1465−1466.
(33) Dunham, M. J.; Gartenberg, M. R.; Brown, G. W. *Methods in Yeast Genetics and Genomics*, 2015 ed.; Cold Spring Harbor Laboratory Press, 2015.
(34) Junne, T.; Wong, J.; Studer, C.; Aust, T.; Bauer, B. W.; Beibel, M.; Bhullar, B.; Bruccoleri, R.; Eichenberger, J.; Estoppey, D.; Hartmann, N.; Knapp, B.; Krastel, P.; Melin, N.; Oakeley, E. J.; Oberer, L.; Riedl, R.; Roma, G.; Schuierer, S.; Petersen, F.; Tallarico, J. A.; Rapoport, T. A.; Spiess, M.; Hoepfner, D. *J. Cell Sci.* **2015**, *128*, 1217−1229.

https://dx.doi.org/10.1021/acs.jnatprod.9b00826
J. Nat. Prod. 2020, 83, 965−971